PROCEEDINGS REPRINT

SPIE—The International Society for Optical Engineering

Reprinted from

Propagation Engineering

28–30 March 1989
Orlando, Florida

Volume 1115

Multi-wavelength transmittance through falling snow

D. L. Hutt, L. R. Bissonnette and D. St. Germain

Defence Research Establishment Valcartier
P. O. Box 8800 Courcelette, Quebec, G0A 1R0, Canada

ABSTRACT

//Measurements of transmittance through falling snow were made in the visible, 3-5 μm and 8-12 μm bands along a 540 m path. In the visible, measurements were made for both a narrow (0.05 mrad) and wide (3mrad) transmitted beam detected by a common receiver. The apparent path averaged extinction, derived from the transmittance measurements using the Beer-Bouguer law, was found to be dependent upon wavelength and transmissometer geometry. The results may be explained by taking into account scattered contributions to the measured transmittance. The results are compared to calculations made with a single-scattering model and a multiscattering model. //

1. INTRODUCTION

Snow particles are much larger than the wavelengths of visible and near-infrared light thus their scattering properties may be described in terms of geometrical optics. The optical cross-section of such large particles is simply two times their geometrical cross-section and is independent of wavelength. This implies that the extinction coefficient of snow is also independent of wavelength since it is proportional to the optical cross-section. However the apparent path averaged extinction coefficient derived from transmission measurements is very much dependent on wavelength and on transmissometer geometry[1,2,3,4]. Differences of up to 43% have been reported[1]. The differences are a result of forward scattered contributions to the measured beam intensity. The relative contribution of the forward scattered energy depends on the wavelength, the beam divergence and the receiver field of view (FOV).

A simple model[5] which takes into account the contribution of diffraction from single-scattering events can explain the observed wavelength and instrument dependence of the apparent extinction for optical depths up to about 2. For greater optical depths multiple-scatterings must be considered. A multiscattering model[6,7] which takes into account forward scattering due to diffraction as well as lateral scattering gives good agreement with the measurements up to an optical depth of 5.4.

2. TRANSMITTANCE MEASUREMENTS

Transmittance measurements in the visible were made with a transmissometer comprised of two transmitted beams detected by a common receiver. One source is a 10 mW HeNe laser with a wavelength of 0.633 μm collimated to a diameter of 2.8 cm with a half-angle divergence of 0.05 mrad. The second source consists of a 200 W quartz halogen incandescent lamp collimated to a 25 cm diameter beam by a Cassegrain telescope with a half-angle divergence of 3 mrad. The collimators are separated by a distance of about 0.5 m. The common receiver has a f/0.8 Fresnel lens objective and photovoltaic silicon detector with a half-angle FOV of 20 mrad. The two beams are modulated at different frequencies and are discriminated at the receiver using lock-in amplifiers. The transmission range is 540 m long so that at the receiver, the narrow beam reaches a diameter of about 10 cm and the wide beam, a diameter of about 3 m. The important distinction is that the receiver captures the entire narrow beam but only a fraction of the wide beam. This results in significant differences in the measured transmittances normalized to the clear-air values.

Infrared transmission measurements were made along a path parallel and 1 m to the side to the visible transmissometer. The source was a 650^0 blackbody collimated to 12 cm diameter using an off-axis parabolic mirror with half-angle beam divergence of 5 mrad. The receiver consists of a 9.1 cm diameter off-axis parabolic mirror which focuses the radiation onto a sandwich InSb-MCT detector sensitive in the 3-5 μm and 8-12 μm bands. The receiver half-angle FOV is 3 mrad. The transmissometer characteristics are summarized in Table 1.

TABLE 1

Characteristics of DREV Transmissometers

Quantity		Narrow Visible	Wide Visible	3-5 μm IR	8-12 μm IR
λ	(μm)	0.63	0.6	3-5	8-12
w_0	(cm)	1.4	9.2	5.9	5.9
ϕ	(mrad)	0.05	3.0	5.0	5.0
R_0	(cm)	12.7	12.7	4.6	4.6
δ	(mrad)	20.0	20.0	3.0	3.0

λ wavelength of transmitted beam
w_0 e-folding radius of the beam at the beam waist
ϕ beam divergence (half-angle)
R_0 receiver aperture radius
δ e-folding angular width of receiver FOV (half-angle)

During transmittance measurements, Particle Measuring Systems probes were used to measure the concentration and size distribution of atmospheric aerosols in the size range 0.15 μm to 32 μm diameter. These data were used to calculate the contribution of aerosols to the observed extinction. It was found that during most snow events recorded, the extinction due to aerosols and fog was negligible compared to the snow extinction. The snowflake crystal type was recorded at half-hour intervals and the airborne mass concentration of the snow was measured continuously (see Refs. 4, 8 and 9).

Figures 1 and 2 show a good example of multispectral transmittance measurements. A clear air period at the end of the snowfall allows for normalization of the four transmissometer channels. Figure 1 shows the transmittance of the narrow and wide visible beams and Fig. 2 shows the transmittance of the 3-5 μm and 8-12 μm bands. Significant differences in transmittance due to transmissometer geometry and wavelength are evident.

3. PHASE FUNCTION MEASUREMENTS

An in-house built polar nephelometer was used to measure the angular scattering function or phase function of falling snow during the transmission measurements. It consists of a 10 mW HeNe laser collimated to a diameter of 2 cm which illuminates a 2 cm^3 sample volume inside a ring-shaped detection chamber. A cross-section of the nephelometer is shown in Fig. 3. Snow crystals are admitted to the sample chamber through an aperture above the sample volume. Light scattered from the snow crystals is detected by 32 detectors located at angular positions from 10^0 to 170^0 in steps of 5^0 (angles are measured with respect to the direction of the laser beam). The detector outputs are recorded simultaneously when it has been determined that a snowflake is in the center of the sample volume thus the nephelometer records the phase function of individual snowflakes. The individual phase functions are recorded by a computer for later analysis. As an example, the average of approximately 2000 phase functions recorded on 1 April 1987 is shown in Fig. 4. The phase function is normalized to unity at 10^0. The DREV polar nephelometer is described in detail in Ref. 10.

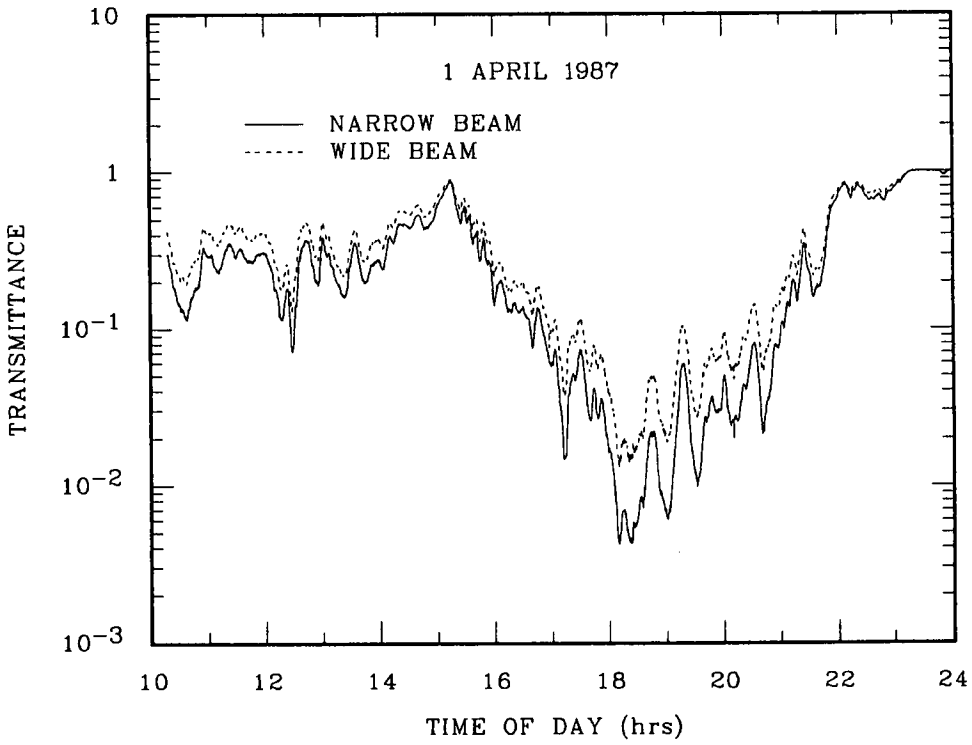

Fig. 1 Transmittance as a function of time for the narrow and wide beam visible transmissometer recorded at DREV on 1 April 1987.

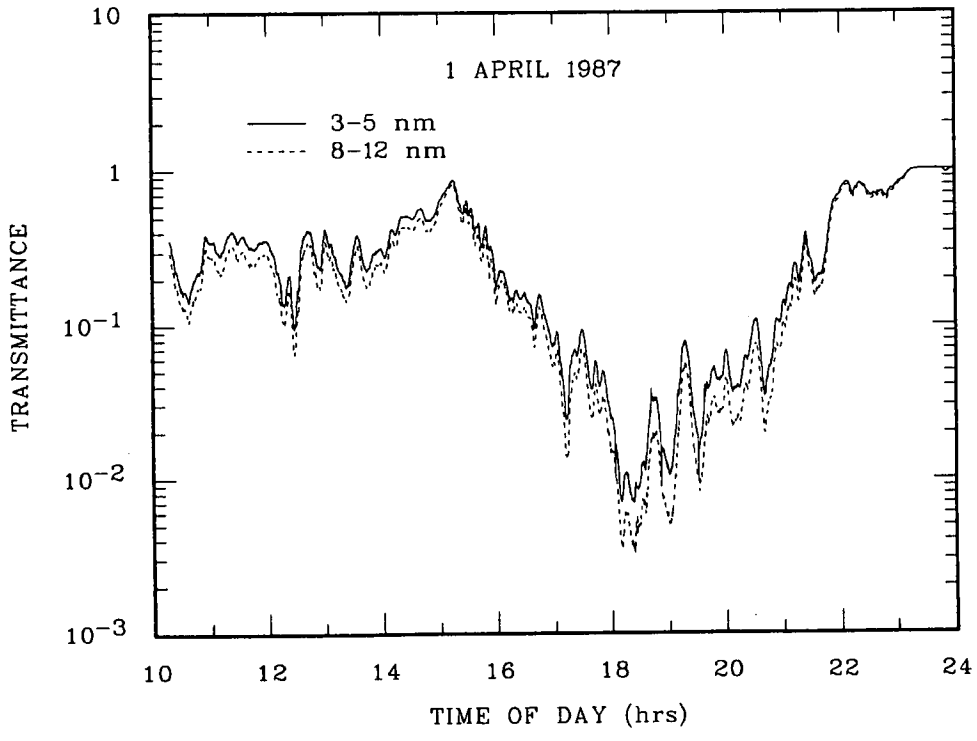

Fig. 2 Transmittance as a function of time for the 3-5 μm and 8-12 μm bands.

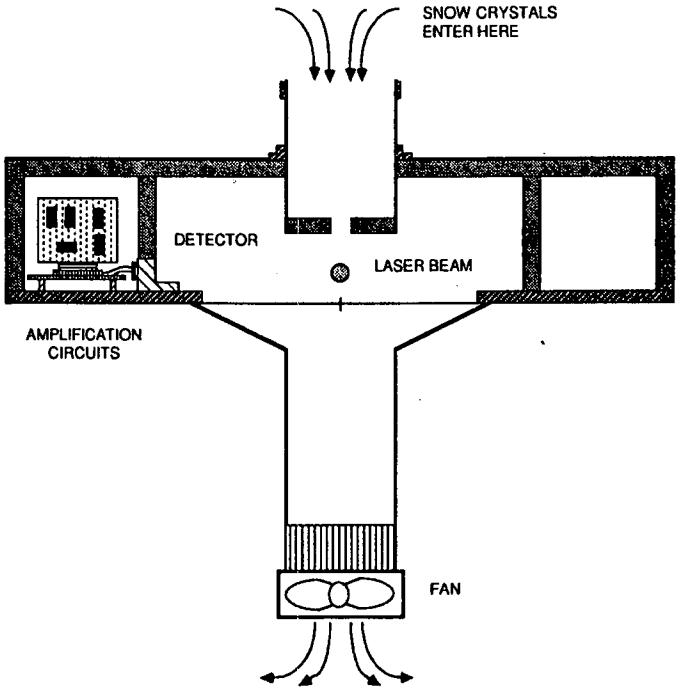

Fig. 3 A cross-section of the ring-shaped nephelometer, perpendicular to the laser beam. One of the 32 detectors which measure light scattered from the laser beam is shown.

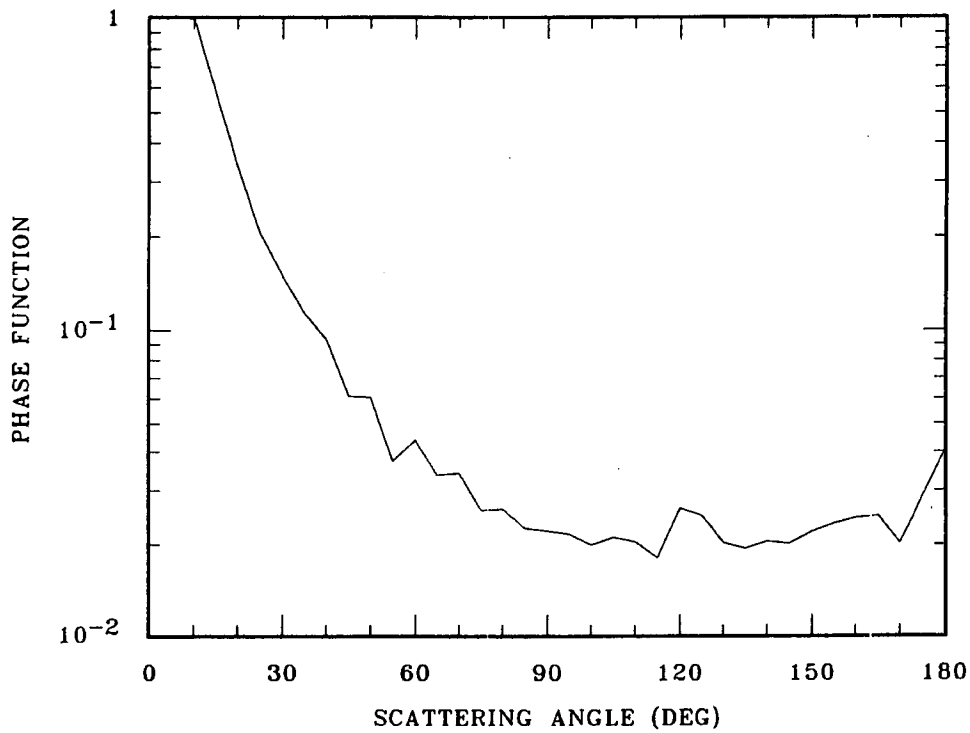

Fig. 4 Average of about 2000 snow phase functions recorded between 10:00 and 24:00 hrs on 1 April 1987.

4. SINGLE-SCATTERING EXTINCTION AND APPARENT EXTINCTION

The extinction coefficient of a medium is defined in terms of the transmittance T as

$$\alpha_{ss} = \frac{ln T}{z} . \qquad [1]$$

where z is the propagation distance. Equation 1 is known as the Beer-Bouguer law. In the derivation of Eq. 1, a light ray scattered once by intervening particles is assumed lost to the beam and does not contribute to the measured transmittance. The extinction coefficient thus defined will be refered to as the single-scattering extinction coefficient. α_{ss} is an intrinsic property of the scattering medium. α_{ss} can be difficult to measure because the measured transmittance may have contributions from forward scattered energy resulting in an underestimate of α_{ss}. The measured transmittance T_m is defined as

$$T_m = \frac{(I_u + I_s)}{I_0} , \qquad [2]$$

where I_0 is the beam intensity when $\alpha_{ss} = 0$, I_u is the unscattered intensity and I_s is the intensity component that has been scattered to the receiver. The definition of α_{ss} given by Eq. 1 is only valid if I_s=0. However in practical measurements I_s is finite and depends in a complex way on the FOV of the receiver, the divergence of the beam, the phase function of the aerosol and on α_{ss}. The extinction coefficient derived from the measured transmittance T_m will be refered to as the apparent extinction coefficient α_a defined as

$$\alpha_a = \frac{ln T_m}{z} . \qquad [3]$$

If the scattered contributions to T_m can be calculated then it should be possible to correct measured values of α_a to get α_{ss}. α_{ss} should be independent of instrumentation and, for large particles such as snowflakes, should be independent of wavelength.

Figure 5 shows the apparent extinction of the wide beam visible transmissometer plotted against that for the narrow beam transmissometer for the snowfall of 1 April 1987. The extinction values range from 0 to 10 km^{-1} which corresponds to a heavy snowfall. Since the measurements were made at practically the same wavelength these results indicate the influence of the beam divergence. There is almost a linear relationship between the coefficients with a slope of 0.79. The wide-beam extinction values are less than those of the narrow-beam due to greater scattered contributions to the wide-beam transmittance. This is a result of the larger scattering volume illuminated by the wide-beam and the greater magnitude of I_s relative to I_u for the wide-beam. Figure 6 is similar to Fig. 5 but shows the apparent extinction of the 3-5 μm band versus the 8-12 μm extinction. Here the measurements were made with the same transmissometer so that the graph shows the wavelength dependence of the apparent extinction. The 3-5 μm extinction is less than that of the 8-12 μm band because the forward scattering diffraction peak of the snowflakes is narrower at 3-5 μm and thus contributes relatively more to the measured transmittance. In Figs. 5 and 6 a dashed line indicates the one to one relationship that is predicted by theory for the single-scattering extinction α_{ss}.

5. SINGLE-SCATTERING CORRECTION

For particles with diameters D larger than the wavelength λ, the scattering phase function is dominated by the forward diffraction peak. For a sphere the angular width of the diffraction peak is $1.22\lambda/D$. Wiscombe and Mugnai[11] have shown that the forward scattering peak of an ensemble of large randomly oriented irregularly shaped particles is similar to that of spheres of equal cross-sectional area. Bohren and Koh[12] showed that randomly oriented spheroids with large aspect ratios have an even more pronounced forward scattering peak than spheres of equivalent cross-sectional area. For our purposes the diffraction peak of an ensemble of snowflakes will be modeled by that of a sphere of some effective radius r. Several models[2,5,13,14] have been proposed to describe the contribution of diffraction to the measured transmission. The Mill and Shettle[5] model will be used here. In their model the single-scattered irradiance I_s collected by

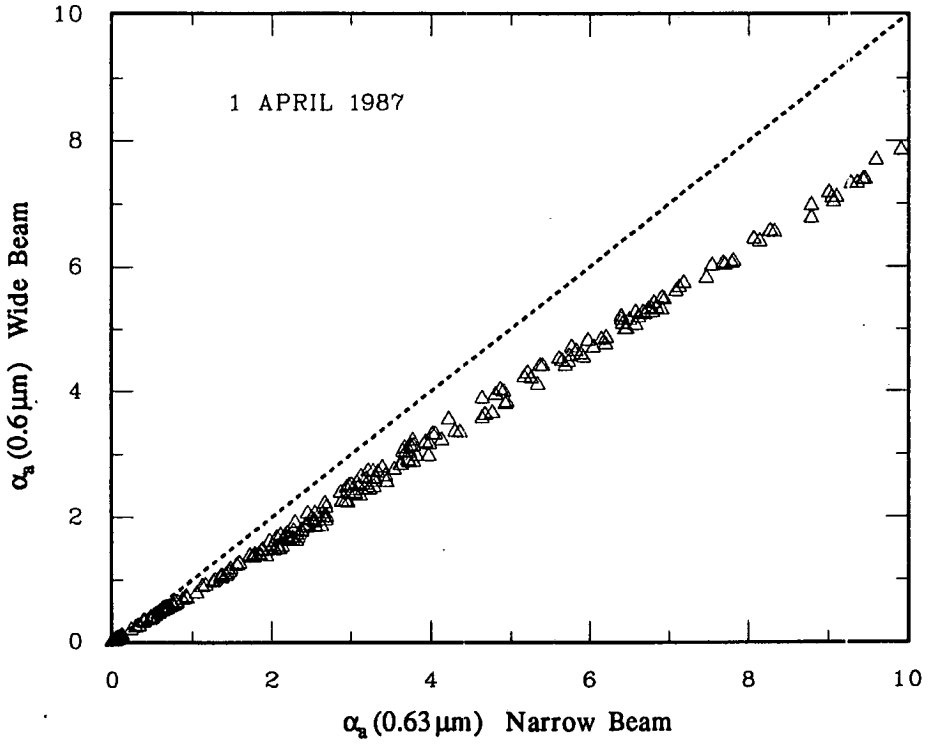

Fig. 5 Apparent visible extinction α_a (0.6 μm) as measured with the wide-beam transmissometer versus that for the narrow-beam. The differences are due to the effect of the beam width.

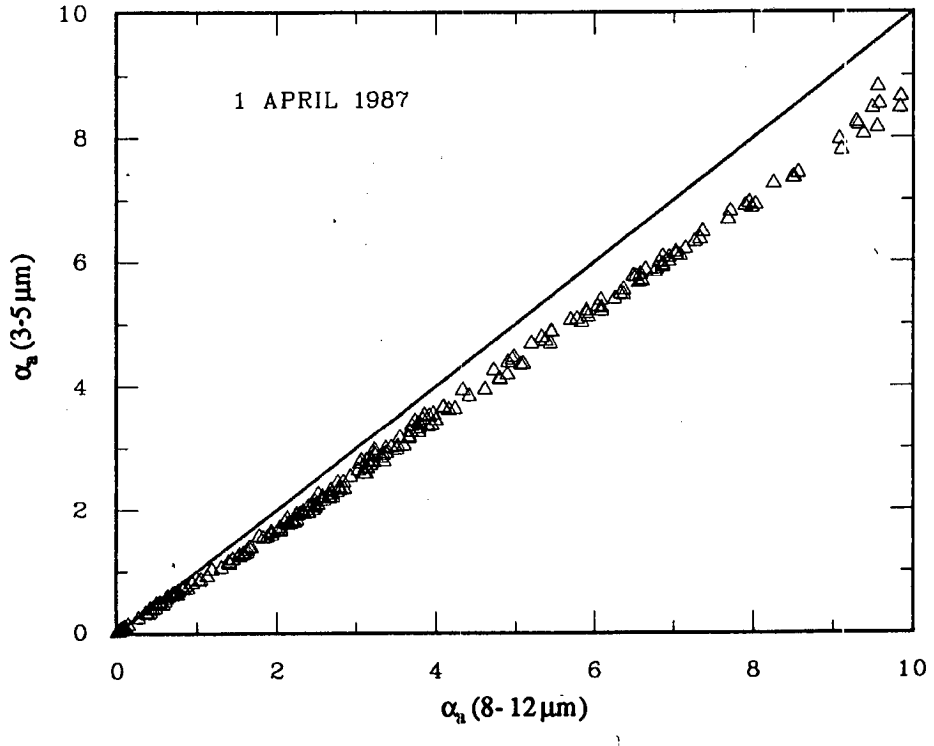

Fig. 6 α_a (3-5 μm) versus α_a (8-12 μm). The measurements were made simultaneously with the same transmissometer thus the graph shows the effect of wavelength on α_a.

the receiver is found by integrating the contributions from all the space common to the beam and the receiver FOV. An expression for T_m is derived in terms of the unscattered transmittance T:

$$T_m = T[1 - 2\pi w \ln T \int_0^{\delta'}\int_0^{\phi'} P_d(\delta+\phi)f(\delta)g(\phi)d\delta\, d\phi] , \qquad [4]$$

where w is the single-scattering albedo, $f(\delta)$ the receiver FOV sensitivity function, $g(\phi)$ the angular beam intensity function and $P_d(\theta)$ a function that approximates the forward diffraction peak of the phase function. For these calculations $P_d(\theta)$ was

$$P_d(\theta) = \frac{\chi^2}{4\pi}\left[\frac{2J_1(\chi\sin\theta)}{\chi\sin\theta}\right]^2 \quad \text{for } \sin\theta_1 < 0.610\frac{\lambda}{r} , \qquad [5]$$

where J_i is the i^{th}-order Bessel function of the first kind, χ is the particle size parameter $2\pi r/\lambda$ and θ_1 is the angle corresponding to the first zero of J_1. Only the scattering contribution of the diffraction peak is considered in the calculation so $P_d(\theta)$ is taken to be zero for $\theta > \theta_1$. For wavelengths on the order of microns and snowflake effective diameters on the order of millimeters the angular width of the forward scattering peak is on the order of milliradians. Since the beam divergence and receiver FOV of the transmissometers are also on the order of milliradians the integrand in Eq. 4 can have a large value with the result that forward scattering may have a great effect on transmission measurements.

The parameters of Table 1 were used to calculate T as a function of T_m using Eqs. 4 and 5. Equation 4 is transcendental and must be solved iteratively for T. The snowflake effective radius used was 500 μm. This value for r was determined empirically by calculating values of T_m for the different transmissometer configurations based on a given value of T and choosing the value of r that gave the best agreement with the observations. 500 μm is very close to the estimated mean radius of snow crystals observed during the snowfall of 1 April 1987. The effect of the single-scattering correction on the apparent extinction is shown in Figs. 7 and 8. The resultant values of α_{ss} approximate much better the one-to-one relationship predicted by theory than the apparent extinction shown in Figs. 5 and 6. For both the visible and IR measurements the agreement is excellent up to extinction values of 4 km^{-1} which corresponds to an optical depth of about 2.

6. MULTIPLE-SCATTERING CORRECTION

For small values of extinction the probability of energy reaching the receiver as a result of multiple-scattering is quite low. However for higher extinction, multiple-scattering becomes significant. In the single-scattering model, light rays were scattered within the narrow forward diffraction peak of an equivalent sphere with zero probability of being scattered at larger angles. In order to model the effect of higher orders of scattering, a more realistic representation of the phase function is required. Indeed diffraction accounts for only 50% of the energy scattered by a large sphere in the geometrical limit thus for a non-absorbing sphere a great deal of energy is scattered at angles outside of the forward peak. It is likely that the degree of lateral scattering is even greater for snowflakes due to scattering by their very fine structures.

The Bissonnette multiscattering propagation model[6,7] will be used here to correct the measured extinction values. The model is a paraxial approximation to the radiative transfer equation. Its principle feature is the representation of the power flux in the lateral direction by a diffusion process. The model is described in detail in Ref. 6. The model requires as input three transmissometer parameters: the wavelength λ, the beam radius w_0 and the divergence ϕ; two receiver parameters: the aperture radius R_0, the 1/e width of the Gaussian function fitted to the receiver FOV profile; and two medium parameters; the single-scattering extinction α_{ss} and the single-scattering albedo w. Two additional quantities are required to characterize the phase function. One is the 1/e width θ_d of a Gaussian function fitted to the forward peak and the other, the average sine of the forward scattering angle $\langle\sin\theta^+\rangle$.

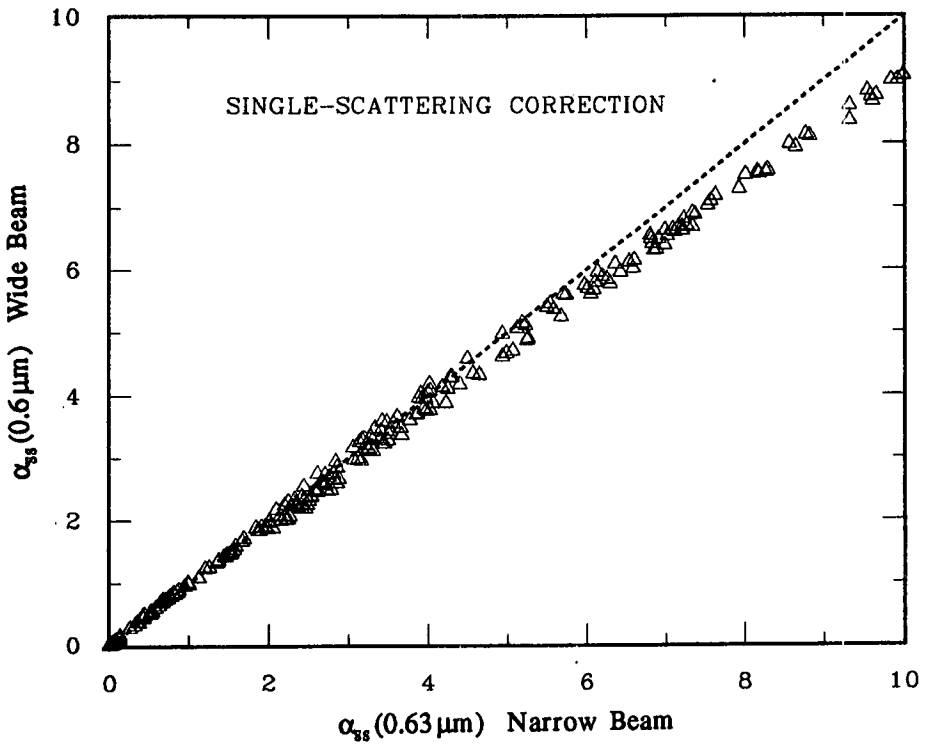

Fig. 7 Single-scattered extinction α_{ss} as derived from the measured visible transmittance using the single-scattering correction. The α_{ss} values should be independent of the instruments.

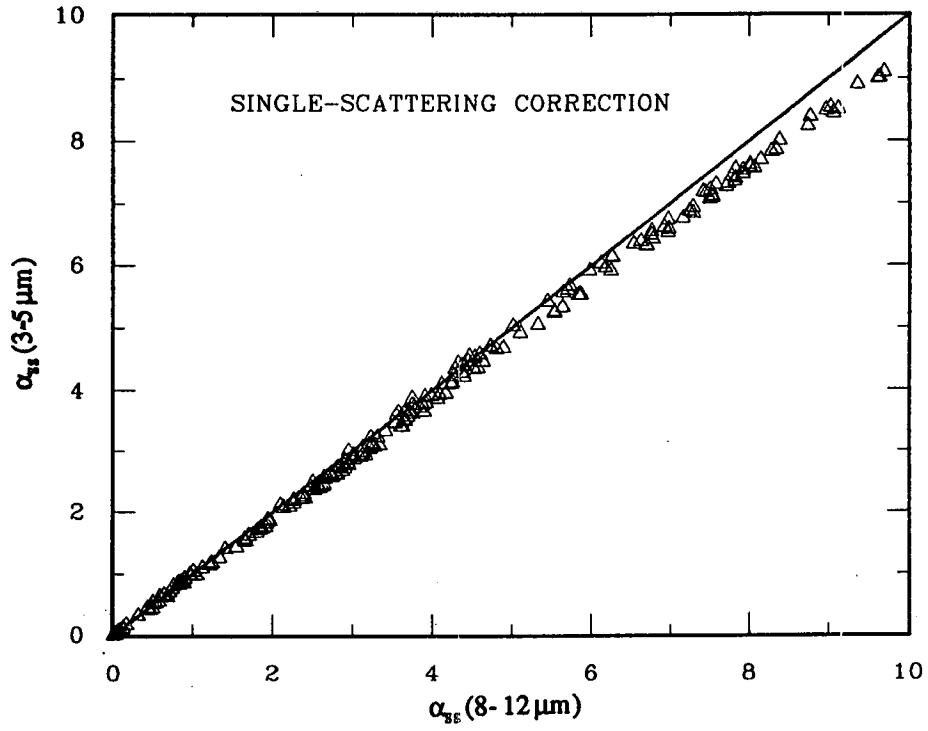

Fig. 8 α_{ss} derived from the IR transmittance using the single-scattering correction. The α_{ss} of snow should be independent of wavelength because the snowflakes are much larger than λ.

θ_d was estimated by fitting a Gaussian function to the diffraction peak phase function defined by Eq. 5 and requiring that the solid angle integrals of the two functions be equal. The result is

$$\theta_d = 0.291 \frac{\lambda}{r} . \qquad [6]$$

According to Eq. 6, θ_d is proportional to the ratio of λ and the equivalent sphere radius r. The second phase function parameter $<\sin\theta^+>$ is defined as

$$<\sin\theta^+> = \int_0^{\pi/2} \sin\theta\, P(\theta) d\theta \Big/ \int_0^{\pi/2} P(\theta) d\theta . \qquad [7]$$

Since the integrals in Eq. 7 are carried out from 0 to $\pi/2$, the entire forward half of the phase function must be considered. We define a phase function $P(\theta)$ that is the sum of the diffraction peak $P_d(\theta)$ and another component $P_m(\theta)$, ie.

$$P(\theta) = \begin{cases} cP_d(\theta)+P_m(\theta) & \theta < \theta_1 \\ P_m(\theta) & \theta > \theta_1 \end{cases} \qquad [8]$$

$P_m(\theta)$ represents the contributions of all scattering effects other than diffraction by the equivalent sphere and c is a constant. The nephelometer measurement shown in Fig. 4 should be a good approximation to $P_m(\theta)$. Unfortunately Eq. 7 cannot be evaluated because $P_m(\theta)$ is not resolved for small angles by the nephelo meter and thus cannot be normalized. However, Bissonnette[15] has shown that $<\sin\theta^+>$ is proportional to λ/r. The constant of proportionality was then determined empirically by comparing model predictions of T_m for the different transmissometers to the measured values. The following relation gives good results for all cases studied:

$$<\sin\theta^+> = 2 \frac{\lambda}{r} . \qquad [9]$$

The multiscattering model was used to correct the measured T_m to get the single-scattering extinction α_{ss}. In the calculations r was set to 400 μm. The results for the test case of 1 April 1987 are shown in Figs. 9 and 10. In Fig. 9, the values of α_{ss} derived from the wide and narrow beam visible transmittance measurements are virtually identical up to an extinction of 10 km^{-1} which corresponds to an optical depth of 5.4. Thus the results of the multiscattering correction are in agreement with theory over a wide range of optical depths. It is interesting to note that both models require very little correction for transmittance measured with the narrow beam transmissometer. In terms of extinction there is only about a 5% difference between α_a and α_{ss} calculated for an optical depth of 5. This is easily understood because the receiver captures the entire beam with the result that the unscattered component of the received power is much greater than the forward scattered component hence the effect of forward scattering on the measured transmittance is small.

Figure 10 shows α_{ss} derived from the IR transmittance values. The data points do not fall exactly on the identity line indicating insufficient correction. The results are only slightly better than the single-scattering correction shown in Fig. 8. Two phase function parameters are required for the multiscattering correction, both of which must be estimated. This could be the reason that the model worked better for the visible trasmissometers than for the IR. Similar results were obtained for three other data sets, two of which were measured by an independent group[16] at the Naval Research Laboratory, Washington D.C.

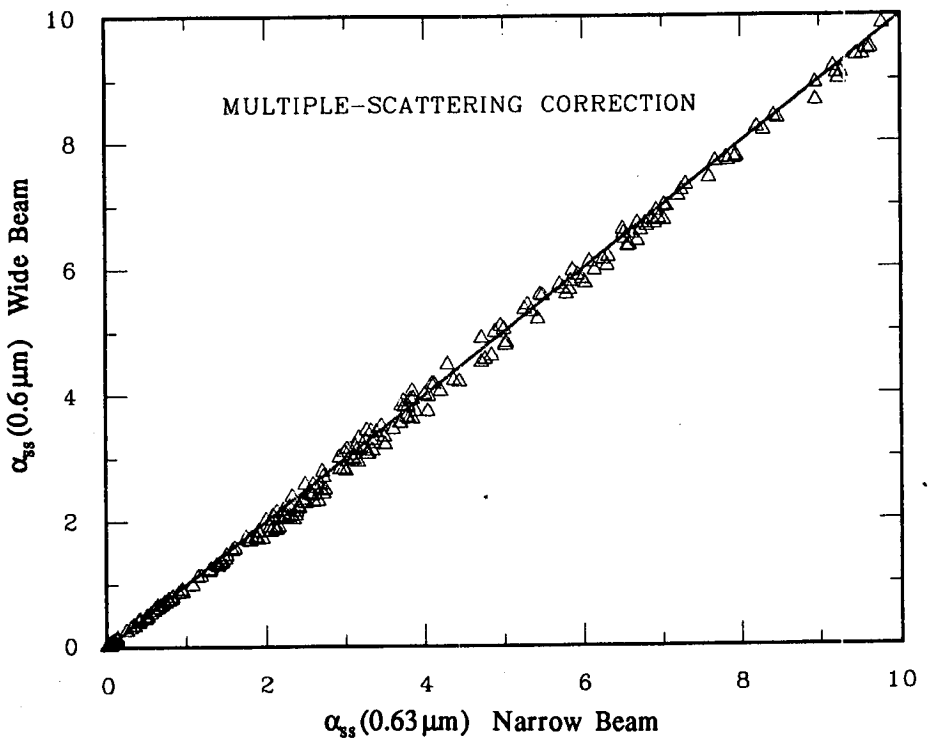

Fig. 9 Single-scattered extinction α_{ss} as derived from the measured visible transmittance using the multiscattering correction.

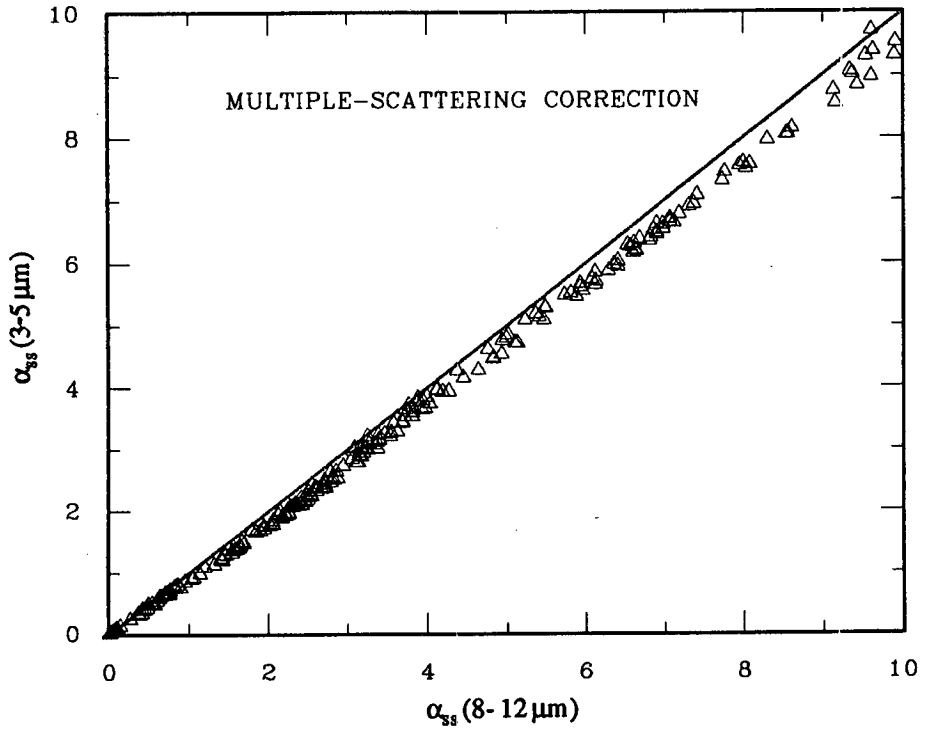

Fig. 10 α_{ss} derived from the IR transmission measurements using the multiscattering correction.

7. CONCLUSIONS

Simultaneous measurements of visible transmittance through falling snow using a dual-beam transmissometer have shown that forward scattered contributions to the measured transmittance are much greater for the wide beam than for the narrow beam. Measurements of IR transmittance in the 3-5 μm band and 8-12 μm band made with the same transmissometer showed that the 3-5 μm transmittance is always greater than that of the 8-12 μm which is contrary to the theoretical requirement that the extinction coeffecient of snow be independent of wavelength in the IR region. Both of these observations can be explained in terms of forward scattering contributions which depend on the snow phase function, the extinction coefficient and the design of the transmissometer. Two models were used to derive the single-scattering extinction coeffecient from the measured transmittances. A single-scattering model[5] which takes into account the forward scattered light from the prominent snow diffraction peak provided good results up to an optical depth of about 2. A multiscattering model[6] was also used. It requires two characteristic parameters of the snow phase function; the width of the forward diffraction peak and the average sine of the forward scattering angle. For the visible transmission data the multiscattering correction gave excellent results up to an optical depth of 5.4. For the IR data both models gave reasonably good results.

8. REFERENCES

1. Sola, M.C. and Bergmann, R.J., "Multi-spectral propagation measurements through snow", Technical Digest, Topical Meeting on Optical Propagation Through Turbulence, Rain and Fog, Optical Society of America, Washington D.C., 1977.
2. Seagraves, M.A., "Visible and infrared extinction in falling snow", Appl. Opt., Vol. 25, pp. 1166-1169, 1986.
3. Winchester,L.W. Jr., Gimmestad, G.G. and Lee, S.M., "Transmission of visible and infrared radiation in falling and blowing snow", Proceedings of SNOW Symposium III, Cold Regions Research and Engineering Laboratory, Hanover, New Hampshire, pp. 69-83, 1983.
4. Hutt, D.L., Bissonnette, L.R. and St. Germain, D., "Extinction of infrared and visible radiation due to airborne snow", DREV Report R-4414/86, 1986.
5. Mill, J.D. and Shettle, E.P. "A preliminary LOWTRAN snow model", Proceedings of SNOW Symposium II, Cold Regions Research and Engineering Laboratory, Hanover, New Hamshire, pp. 239-250, 1982.
6. Bissonnette, L.R., "Multiscattering model for propagation of narrow light beams in aerosol media", Appl. Opt., Vol. 27, pp.2478-2484, 1988.
7. Bissonnette, L.R., et al., "Transmitted beam profile, integrated backscatter, and range resolved backscatter in inhomogenous laboratory water droplet clouds", Appl. Opt., Vol. 27, pp. 2485-2494, 1988.
8. Lacombe, J., "Technique for measuring the mass concentration of falling snow", SPIE Proceedings Vol. 414, pp. 17-21, 1983.
9. Hutt, D.L., Bissonnette, L.R. and Oman, J., "The measurement of airborne snow mass concentration", DREV Report R-4454/87, 1987.
10. St. Germain, D. and Bissonnette, L.R., "A polar nephelometer for snowflake phase function study", DREV Report R-4500/88, 1988.
11. Wicombe, W. and Mugnai, A., "Exact calculation of scattering from moderately-nonspherical T_n particles: comparison with equivalent spheres", Light Scattering by Irregularly Shaped Particles, pp. 141, Plenum Press, New York, 1979.
12. Bohren, C.F. and Koh, G., "Forward-scattering corrected extinction by nonspherical particles", Appl. Opt. 24, pp. 1023-1029, 1985.

13. Zuev, V.E., Propagation of infrared and visible radiation in the atmosphere, translated from the Russian by D. Lederman, Wiley, Toronto, 1974.

14. Hodkinon, J.R. and Greenleaves, L., "Computations of light scattering and extinction by spheres according to diffraction and geometrical optics", J. Opt. Soc. Am., 53, pp. 577, 1963.

15. Bissonnette, L.R., Hutt, D.L. and St. Germain, "Forward scattering effect on the extinction coefficient of airborne snow: measurements and calculations", DREV Report R-4501/88, 1988.

16. Curcio, J.A. and Lebow, P., "Spectral transmittance measurements at SNOW-TWO", SNOW-TWO Data Report, Vol. 2, Cold Regions Research and Engineering Laboratory, Hanover, New Hamshire, pp. 3-16, 1984.